BMR Journal of Australian Geology & Geophysics, 9, 297-302

Australian long-wavelength magnetic anomalies

Peter Wellman[1], A.S. Murray[1], & M.W. McMullan[2]

A long-wavelength magnetic anomaly map is derived from near-surface observations. The data can be continued upward for comparison with maps derived from satellite data. Compared with a map from 400-km altitude observations of the MAGSAT satellite, the highs and lows are in a similar geographic position, but the MAGSAT map is smoothed, possibly by uncorrected variations in satellite altitude. The long-wavelength magnetic anomalies have no significant correlation with heat flow or seismically measured crustal thickness, and have an amplitude higher than that expected for a non-magnetic sediment. In central and western Australia, magnetic highs are spatially associated with crustal block boundaries defined by elongate, high-amplitude, associated gravity highs and lows. Consequently, the long-wavelength magnetic anomalies are thought to be caused by rocks of high magnetisation in the upper or lower crust.

Introduction

The long-wavelength magnetic field is important because of its potential to give significant new information on long-wavelength crustal properties that is independent of other methods. Magnetic measurements on POGO and MAGSAT satellites have recently been used to determine long-wavelength magnetic anomalies over Australia (Mayhew & others, 1980; Langel & others, 1982).

In this study the long-wavelength anomalies calculated from near-surface magnetic measurements are compared with the satellite long-wavelength anomalies, and are used to investigate the lithospheric source of the anomalies. Long-wavelength magnetic observations have previously been described by Dooley (1979), Dooley & McGregor (1982) and Mayhew & others (1980).

MAGSAT satellite magnetic anomaly map

Figure 1 gives the MAGSAT satellite magnetic anomaly field at 400 km altitude with a 2° grid (Langel & others, 1982). The profiles are at a 7° angle from north to south, with average altitude varying from 349 km to 467 km. The regional field used is MGST 4/81, a 13th degree and order spherical harmonic model derived from world MAGSAT measurements (Langel & others, 1981).

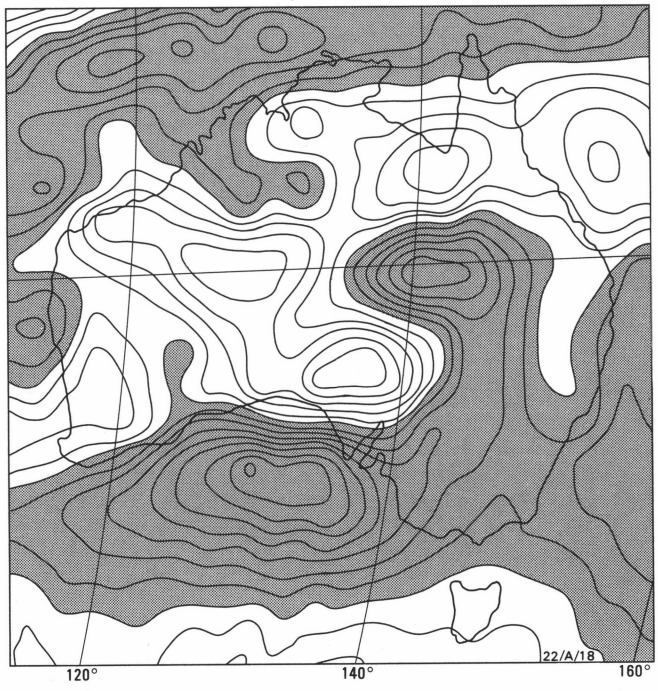

Figure 1. MAGSAT anomaly map, 200 km grid, 400 km (349–467 km) altitude, 2 nT contour interval.
Negative anomalies are stippled (after Langel & others, 1982).

Aeromagnetic long profiles

Numerous profiles across Australia of the total magnetic field were flown between 8 November 1975 and 8 March 1976, using a Bureau of Mineral Resources aeromagnetic aircraft (Dooley & McGregor, 1982) (Fig. 2). Flights were at 3 km altitude with one exception, and mainly between 2100 and 0600 hours UT. The magnetic field was measured with a proton precession magnetometer and paper chart recorder. The charts were subsequently digitised at 1 minute intervals, which is equivalent to an average horizontal ground distance of 5 km. Navigation was by normal aircraft navigation aids and maps. Anomalies were corrected for the secular variation between flight date and 1980.0 with the model of McEwin & others (1981). This secular variation model is a polynomial derived mainly from repeat readings at 62 first-order magnetic stations within Australia. The regional field model MGST 4/81 was used for the 1980.0 field, so that the anomalies would have the same regional as those of Langel & others (1982).

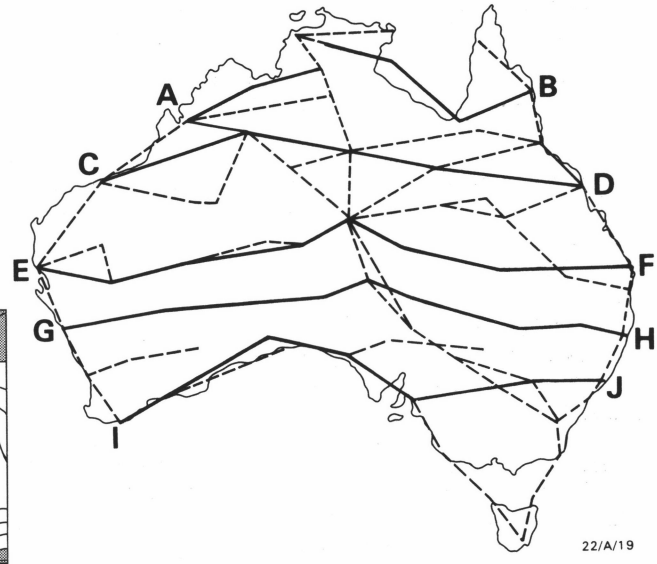

Figure 2. Flight lines of 1975–1976 long-profile survey.
Profiles in Figure 3 are those shown as solid lines.

During most flights a temporary ground station recorded diurnal variation. However, almost all ground recording stations were near the coast, so the recorded diurnal variation over-emphasised the coastal effect and was often over 1000

[1]Division of Geophysics, BMR
[2] Present address: Learmonth Solar Observatory, Exmouth, Western Australia 6707

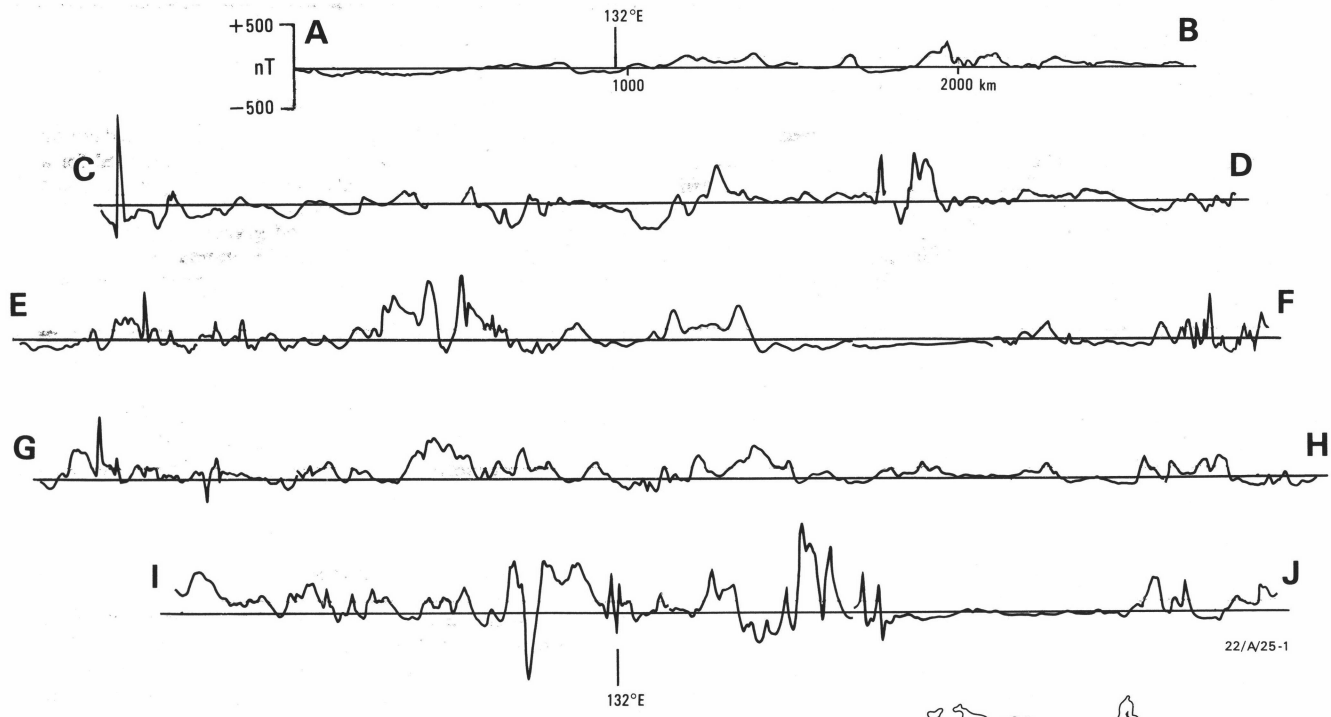

Figure 3. Magnetic anomaly profiles across Australia at 3 km altitude.
Location of profiles is shown in Figure 2.

km from the flight recording. Diurnal corrections were found to decrease rather than increase the consistency of measurements at flight-crossing points, so the diurnal corrections were not used. The 10 368 anomaly values had a mean of −91 nT, which was subtracted from the anomalies to give a zero mean. Figure 3 shows a selection of east-west profiles.

Third-order ground spot readings

From 1967 to 1975 the observatory section of BMR made surface spot readings of three magnetic components over most of Australia (Dooley & McGregor, 1982) (Fig. 4). In the desert area of central and western Australia readings were taken on a grid of 15 minutes (25 km) spacing, using helicopter transport. Over most of Australia they are at approximately 15-km intervals along roads, the roads being spaced approximately 100 km apart. The 7800 readings of total magnetic intensity were made with proton precession magnetometers.

Observations were made during daylight hours. No diurnal corrections have been made. Secular variation corrections from the observation date to 1975.0 have been made by linearly interpolating between three magnetic observatories in the Australian region and approximating the observatory mean-annual-values by a linear change. The changes used between 1967.0 and 1975.0 are for the three observatories: PMG −26 nT, GNA −108 nT, TOO −144 nT.

Secular variation from 1975 to 1980 is from McEwin & others (1981), and the regional magnetic field used for 1980.0 is MGST 4/81. To get a zero mean, 41 nT has been added to the anomalies.

Comparison of zero-level of data sets

Contour maps of third-order anomalies are generally similar in level and form to maps of long-profile anomalies. The exception is the northwestern corner of Australia, where the

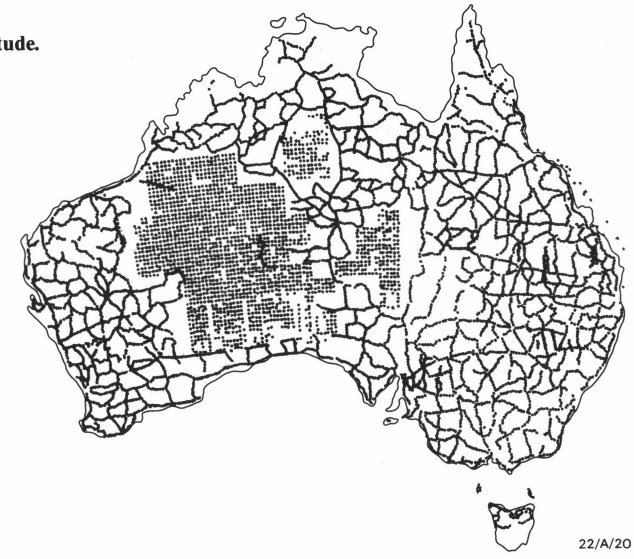

Figure 4. Station distribution of third-order survey of 1967—1975.

third-order anomalies seem to be about 30 nT more negative. The discrepancy may be due to incorrect secular variation correction in that area.

Diurnal variation during daylight hours is up to 50 nT in Australia (McEwin & others, 1981). The mean long-profile field of −91 nT and the mean third-order field of −41 nT are therefore much more negative than can be explained by diurnal variation and the difference in local time between the satellite and near-surface observations. These differences in mean anomaly may be due to errors in the secular and regional fields.

Comparison of near-surface and satellite anomalies

Near-surface composite maps were prepared, the third-order and long-profile data being used together to obtain the maximum number of observations. The data were gridded, continued upward, and contoured on the CSIRONET Cyber 7600 computer (Murray, 1977). Figure 5 shows the anomalies

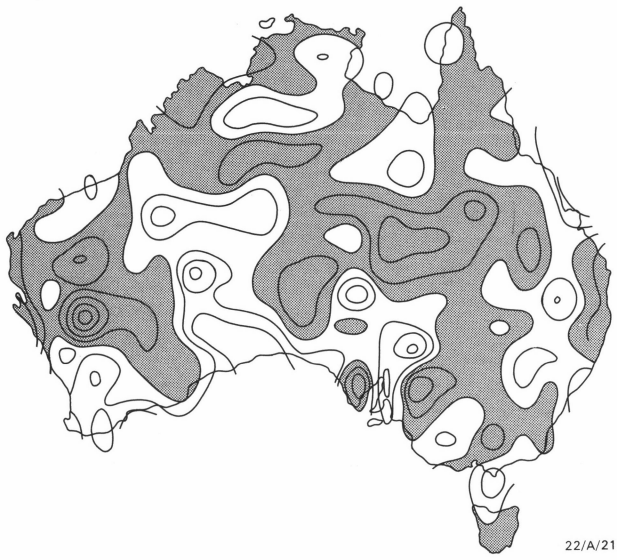

Figure 5. Anomalies from third-order plus long-profile surveys, 200 km grid, 1.5 km altitude, 50 nT contour interval.

with the same size grid as the MAGSAT map of Figure 1 (200 km), but with a 1.5 km rather than 400 km mean altitude. The position and relative amplitude of the anomalies on these two maps are so similar that both sets are likely to be mainly due to a real geographic variation in magnetic anomaly.

Figure 6 has been prepared from a 100 km grid (Fig. 7) continued upward to 400 km by applying the upward-continuation coefficients for a plane (Henderson, 1960) to the 100-km grid points and taking the mean of four adjacent grid points to give 200 x 200 km mean values, like those of the MAGSAT map of Figure 1. Upward continuation of a 100 km grid gives edge effects of smaller geographic extent than those resulting from a 200 km grid. The use of plane rather than spherical upward continuation is thought to lead to errors of no more than 5 per cent in amplitude at 400 km altitude (Vints & others, 1970; J.C. Dooley, personal communication). High-amplitude short-wavelength components in the third-order and long-profile data are suppressed by both the coarse grid averaging and the upward continuation, so they should have a negligible effect on the values of the 200 km grid at 400 km altitude. Long-wavelength anomalies should be preserved by the gridding and upward continuation.

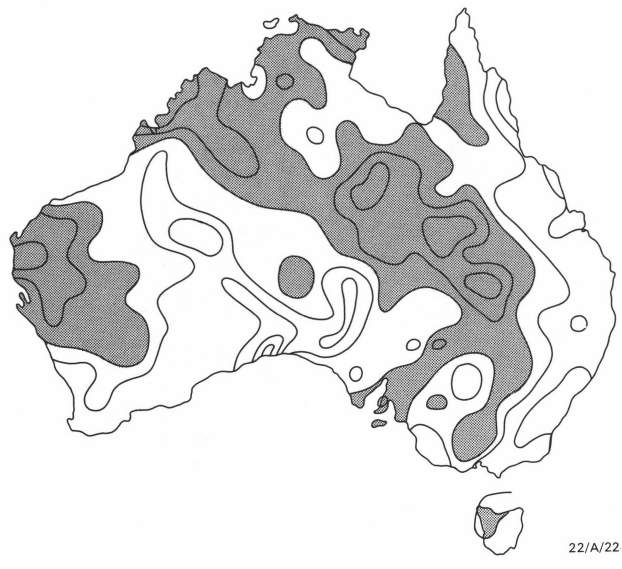

Figure 6. Anomalies from third-order plus long-profile surveys, 200 km grid, 400 km altitude, 10 nT contour interval.

Near the centre of Australia the anomalies calculated for 400 km from near- surface data have a wavelength of about half and an amplitude about twice those shown on the MAGSAT map. This amplitude and wavelength difference between near-surface and satellite data is also found if near-surface data are first gridded at 200 km and then continued upward to 400 km altitude. The difference in amplitude and wavelength is attributed to smoothing of the MAGSAT map caused by both the considerable difference in altitude of the satellite passes and adjacent profiles having different zero level because the fitted and subtracted quadratic functions do not precisely remove the effects of external fields. An amplitude discrepancy that is smaller but in the same direction is found between near-surface and MAGSAT anomalies over Canada (fig. 2a, b of Langel & others, 1980) and the USA (von Frese & others, 1982; Won & Son, 1982).

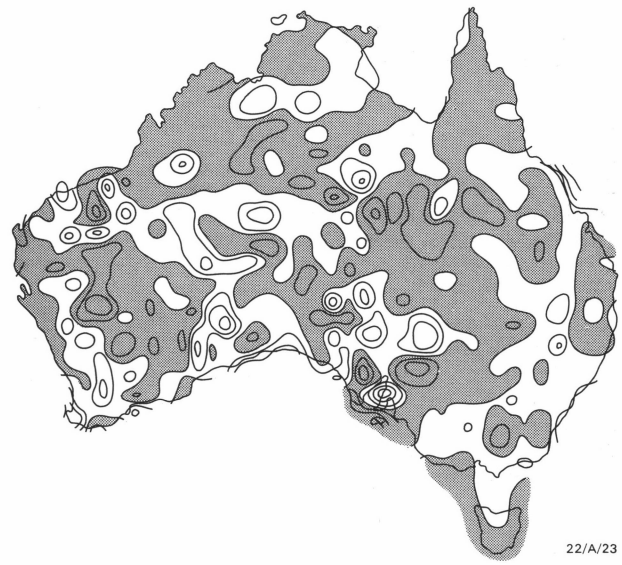

Figure 7. Anomalies from third-order plus long-profile surveys, 100 km grid, 1.5 km altitude, 100 nT contour interval.

Cause of long-wavelength magnetic anomalies

Long-wavelength magnetic anomalies could be caused by either long-wavelength magnetic sources or many adjacent short-wavelength sources. The magnetic sources could be abnormally high or abnormaly low magnetisation in either the upper or lower part of the crust.

Possible variation in thickness of the magnetised lower crust

If the lower crust has uniform magnetisation, then regional variation in heat flow should show a negative correlation with long-wavelength magnetic anomalies, the hotter crust having a shallower Curie point and so being less magnetic. A composite heat-flow map (Fig. 8) does not show the expected correlation with Figure 5: in particular, eastern South Australia has high heat flow and high magnetic anomaly, and the central part of Western Australia has low heat flow and low magnetic anomaly. Figure 9 shows that there is no significant correlation between mean heat flow at the better (>333) heat-flow sites of Cull (1982) and the 2° grid magnetic anomaly (Fig. 5).

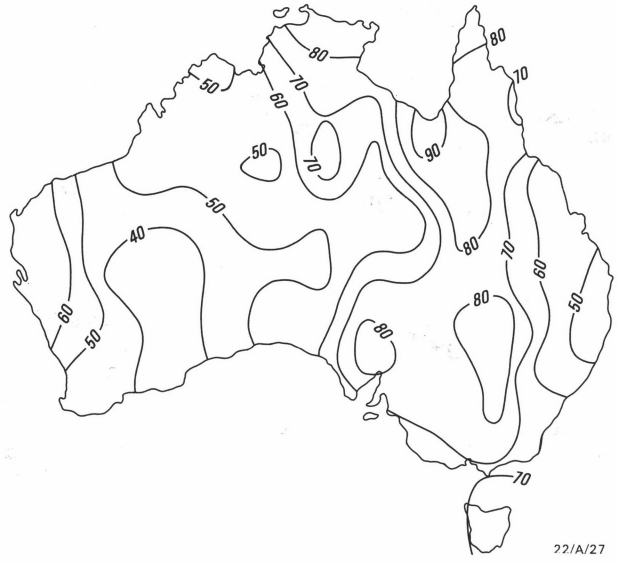

Figure 8. Heat flow in Australia, 3° grid, 10 mW.m^{-2} contour interval (after Cull & Conley, 1983).

If the crust has uniform magnetisation, but varies in thickness, then the thicker crust will be more magnetic. Seismic refraction determinations of crustal thickness, using amplitudes and synthetic seismograms (Wellman, 1982; Finlayson & others, 1984), do not show the expected positive correlation with long-wavelength magnetic anomalies (Fig. 10).

Both the above comparisons are with the observed magnetic anomaly, not the intensity of magnetisation of the magnetic source model. Mayhew & others (1980) showed that most of the long-wavelength anomalies are not significantly offset from their source body.

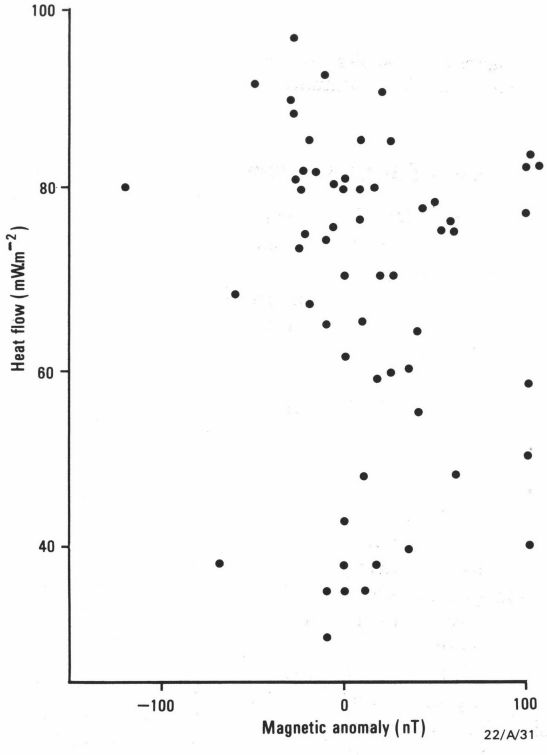

Figure 9. Correlation between heat flow and magnetic anomaly (2° grid).

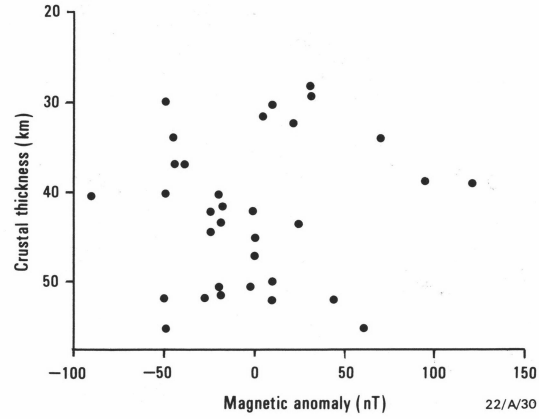

Figure 10. Correlation between seismic crustal thickness and magnetic anomaly (2° grid).

As heat flow and crustal thickness do not have a significant correlation with long-wavelength magnetic anomalies, the long-wavelength magnetic anomalies are unlikely to be caused by variation in the thickness of the magnetic layer in the lower crust.

A cause of low magnetic anomalies in sediments within the upper crust

The major low magnetic anomalies of Figures 1 and 5 are extensive areas of low-amplitude anomaly with a slightly negative mean (Figs. 3, 7, 11) The major areas of low magnetic anomalies in eastern Australia (Figs. 1, 5) correspond in position with the major post-cratonisation sedimentary basins of Phanerozoic age — the Carpentaria, Eromanga, and Murray Basins (Dooley, 1979; Mayhew & others, 1980). The major areas of low magnetic anomaly in western Australia do not overlie single tectonic units, but large parts of them correspond with the major post-cratonisation sedimentary basins of Proterozoic age.

The magnetic anomaly due to the two sedimentary basins has been modelled two-dimensionally, by assuming that the sediments are non-magnetic and that the non-sedimentary rocks underlying the basin have an apparent susceptibility

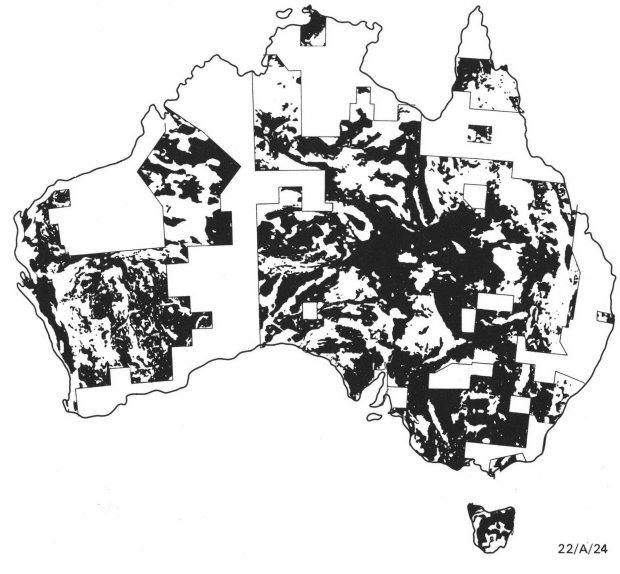

Figure 11. Aeromagnetic anomalies, black negative (from BMR, 1976).

of 0.0016 emu in the c.g.s. system (0.02 in SI system). There are few accurate measurements of mean apparent susceptibility of the uppermost crust. The value used here is that determined for Enderby Land in Antarctica (Wellman, 1983a); this value is likely to be too high, because Enderby Land is deeply eroded (Wellman, 1983b) and within a MAGSAT anomaly high (Ritzwoller & Bently, 1982). At the Earth's surface the calculated peak-to-peak amplitudes of the long-wavelength anomalies that coincide with the basins are 5 nT for the Eromanga Basin, of 3 km depth and 750 km width, and 1 nT for the Canning Basin, which is deeper but more irregular in depth. These anomalies are small compared with those at 1.5 km (Fig. 5) and 400 km (Figs. 1, 6). This suggests that the low magnetic anomalies are not caused principally by lower magnetisation of the sediments relative to the average crust.

Changes in magnitude of crustal magnetisation as a cause of high magnetic anomalies

Amplitudes of long-wavelength anomalies are lower in the Phanerozoic eastern third of Australia than in the Precambrian western two-thirds (Fig. 7). In the eastern third of Australia the long-wavelength magnetic anomalies correlate roughly with areas of exposed basement. In the western two-thirds of Australia the positive magnetic anomalies correlate well with outcropping and subcropping crustal block boundaries (Fig. 12) inferred from analysis of gravity anomaly trends (Wellman, 1976) and from large, adjacent positive and negative gravity anomalies (Wellman, 1978). The ground location of the high magnetic anomalies is shown on the aeromagnetic maps of Australia; data to 1976 are given in Figure 11. The high magnetic anomalies are associated with the high gravity anomalies at one side of the junction of crustal blocks. Both gravity and magnetic anomalies are thought to be due to lower crustal material that has been obducted to near the Earth's surface (Karner & Watts, 1983).

Frey & others (1983) have shown that on a reassembled Gondwanaland the MAGSAT anomalies reduced to poles are continuous across Gondwanaland fragments. This is consistent with a cause of the anomalies in crustal block boundaries as these boundaries predate the break up of Gondwanaland.

Figure 12. Positive magnetic anomalies (1° grid) and crustal block boundaries from gravity anomalies (from Wellman, 1978).

Conclusions

Magnetic anomalies at satellite altitudes can be determined using near-surface observations, provided that the near-surface observations have an accurate datum and the secular variation is known.

These near-surface observations are more useful than MAGSAT anomalies for studies of the lithosphere, because they contain the shorter-wavelength information that is necessary to reliably correlate anomalies with crustal features.

The long-wavelength anomalies in Australia are interpreted here as mainly due to high apparent-susceptibility rock in the upper or lower crust. The rock occurs in areas of basement uplift in eastern Australia and at one side of block boundaries in central and western Australia.

Acknowledgements

I thank J.C. Dooley, A.J. McEwin, P.M. McGregor, G.R. Small, and anonymous reviewers for comments on data reduction and the text, and R.W. Bates and P. Corbett for the drafting.

References

BMR, 1976 — Magnetic map of Australia, residuals of total intensity, scale 1:2 500 000. *Bureau of Mineral Resources, Australia.*

Cull, J.P., 1982 — An appraisal of Australian heat-flow data. *BMR Journal of Australian Geology & Geophysics*, 7, 11–21.

Cull, J.P., & Conley, D., 1983 — Estimates of temperature and heat flow in the sedimentary basins of Australia, *BMR Journal of Australian Geology & Geophysics*, 8, 329–337.

Dooley, J.C., 1979 — A geophysical profile across Australia at 29½S, *BMR Journal of Australian Geology & Geophysics*, 4, 353–359.

Dooley, J.C., & McGregor, P.M., 1982 — Correlative geophysical data in the Australian region for use in the MAGSAT project, *Bulletin of the Australian Society of Exploration Geophysicists*, 13, 63–67.

Frey, H., Langel, R.A., Mead, G., & Brown, K., 1983 — Pogo and Pangea. *Tectonophysics*, 95, 181–189.

Finlayson, D.M., Collins, C.D.N., & Lock, J., 1984 — P-wave velocity features of lithosphere under the Eromanga Basin, eastern Australia, including a prominent mid-crustal (Conrad?) disconformity. *Tectonophysics*, 101, 267–291.

Henderson, R.G., 1960 — A comprehensive system of automatic computation in magnetic and gravity interpretation. *Geophysics*, 25, 569–585.

Karner, G.D., & Watts, A.B., 1983 — Gravity anomalies and the flexure of the lithosphere at mountain ranges. *Journal of Geophysical Research*, 88, 10449–10477.

Langel, R.A., Berbert, J., Jennings, T., & Horner, R., 1981 — MAGSAT data processing: an interim report for investigators. *NASA TM 82160, Nov 1981.*

Langel, R.A., Coles, R.L., & Mayhew, M.A., 1980 — Comparisons of magnetic anomlies of lithospheric origin measured by satellite and airborne magnetometers over western Canada. *Canadian Journal of Earth Sciences*, 17, 876–887.

Langel, R.A., Phillips, J.D., & Horner, R.J., 1982 — Initial scalar magnetic anomaly map from Magsat. *Geophysical Research Letters*, 9, 269–272.

Mayhew, M.A., Johnston, B.D., & Langel, R.A., 1980 — An equivalent source model of the satellite altitude magnetic anomaly field over Australia. *Earth & Planetary Science Letters*, 51, 189–198.

McEwin, A.J., McGregor, P.M., & Small, G.R., 1981 — Total magnetic intensity, Australia, epoch 1980.0, scale 1:10 000 000. *Bureau of Mineral Resources, Australia.*

Murray, A.S., 1977 — A guide to the use and operation of program CONTOR. *Bureau of Mineral Resources, Australia, Record* 1977/17.

Ritzwoller, M.H., & Bentley, C.R., 1982 — MAGSAT magnetic anomalies over Antarctica and the surrounding oceans. *Geophysical Research Letters*, 9, 285–288.

Vints, B.D., Pochtarev, V.I., & Rakhmatulin, R.Sh., 1970 — Method of computing the geomagnetic field upwards in nearrth space. *Geomagnetism & Aeronomy*, 10, 90–98.

von Frese, R.R.B., Hinze, W.J., Sexton, J.L., & Braile, L.W., 1982 — Verification of the crustal component in satellite magnetic data. *Geophysical Research Letters*, 9, 293–295.

Wellman, P., 1976 — Gravity trends and the growth of Australia: a tentative correlation. *Journal of the Geological Society of Australia*, 23, 11–14.

Wellman, P., 1978 — Gravity evidence for abrupt changes in mean crustal density at the junctions of Australian crustal blocks. *BMR Journal of Australian Geology & Geophysics*, 3, 153–162.

Wellman, P., 1982 — Australian seismic refraction results, isostasy and altitude anomalies. *Nature*, 298, 838–841.

Wellman, P., 1983a — Interpretation of geophysical surveys — longitude 45° to 65°E, Antarctica. *In* Oliver, R.L., James, P.R., & Jago, J.B., (editors) Antarctic Earth Science. *Australian Academy of Sciences, Canberra,* 522–526.

Wellman, P., 1983b — Origin and subglacial erosion of part of the coastal highland of east Antarctica. *Journal of Geology*, 91, 471–480.

Won, I.J., & Son, K.H., 1982 — A preliminary comparison of the Magsat data in the continental U.S. *Geophysical Research Letters*, 9, 296–298.